J. Biochem. **141**, 101–112 (2007)
doi:10.1093/jb/mvm008

Functional Significance of Asn-linked Glycosylation of Proteinase 3 for Enzymatic Activity, Processing, Targeting, and Recognition by Anti-neutrophil Cytoplasmic Antibodies

Ulrich Specks[1]*, David N. Fass[2], Javier D. Finkielman[1], Amber M. Hummel[1], Margaret A. Viss[1], Robert D. Litwiller[2] and Cari J. Mcdonald[1]

[1]Thoracic Disease Research Unit; and [2]Hematology Research Unit, Mayo Clinic and Foundation, Rochester, MN 55905, USA

Received November 08, 2006; accepted November 13, 2006; published online December 11, 2006

Proteinase 3 (PR3) is a neutral serine protease stored in neutrophil granules. It has substantial sequence homology with elastase, cathepsin G and azurocidin. PR3 is the target antigen for autoantibodies (ANCA) in Wegener's granulomatosis, a necrotizing vasculitis syndrome. ANCA have been implicated in the pathogenesis of this disease. PR3 has two potential Asn-linked glycosylation sites. This study was designed to determine the occupancy of these glycosylation sites, and to evaluate their effect on enzymatic function, intracellular processing, targeting to granules and recognition by ANCA. We found that glycosylation occurs at both sites in native neutrophil PR3 and in wild type recombinant PR3 (rPR3) expressed in HMC-1 cells. Using glycosylation deficient rPR3 mutants we found that glycosylation at Asn-147, but not at Asn-102, is critical for thermal stability, and for optimal hydrolytic activity of PR3. Efficient amino-terminal proteolytic processing of rPR3 is dependent on glycosylation at Asn-102. Targeting to granules is not dependent on glycosylation, but unglycosylated rPR3 gets secreted preferentially into media supernatants. Finally, a capture ELISA for ANCA detection, using rPR3 glycosylation variants as target antigens, reveals that in about 20% of patients, epitope recognition by ANCA is affected by the glycosylation status of PR3.

Key words: neutrophils, protein processing, post-translational, serine endopeptidases, Wegener's granulomatosis.

Abbreviations: ANCA, anti-neutrophil cytoplasmic antibodies; EGTA, Ethylene glycol bis-2-aminoethyl ether-N,N′,N″,n′-tetraacetic acid; ELISA, enzyme linked immunosorbent assay; HMC-1, human mast cell line-1; HPLC, high pressure liquid chromatography; moAB, monoclonal antibody; MPO, myeloperoxidase; PR3, proteinase 3.

Proteinase 3 (PR3, EC 3.4.21.76) is a neutral serine protease that is stored in granules of neutrophils and monocytes (*1*). PR3 has substantial amino acid sequence homology with elastase, cathepsin G and azurocidin (*2, 3*). Most putative biological functions ascribed to PR3 are dependent on its proteolytic activity. As PR3 is expressed on the surface of activated neutrophils, and its enzymatic substrates include basement membrane proteins, one of the physiologic functions of PR3 may be to facilitate the migration of neutrophils to tissue sites of inflammation (*4–6*). The proteolytic activity of PR3 affects the activation of platelets and endothelial cells (*7, 8*), and modulates the biologic activity of inflammatory mediators such as C1-inhibitor (*9*), interleukin-8 (IL-8) (*10*), tumour necrosis factor-α (TNF-α) (*11, 12*), IL-1β (*12*), and transforming growth factor-β (TGF-β) (*13*). Other potential biologic activities of PR3 such as bactericidal activity (*14*), induction of IL-8 secretion from endothelial cells (*15*), or blockade of neutrophil NADPH oxidase activation (*16*) appear to be independent of its proteolytic activity, suggesting that they are mediated by structural domains distinct from the active site. PR3 has also been implicated in regulating cell proliferation and maturation during haematopoiesis (*17–20*), and its role as target for immunotherapy of myeloid leukaemias is under investigation (*21, 22*).

PR3 is the main target antigen for anti-neutrophil cytoplasmic antibodies (ANCA) in patients with Wegener's granulomatosis (*23*), a systemic autoimmune vasculitis that affects small to medium sized blood vessels and commonly involves the upper respiratory tract, lungs and kidneys. The interactions of ANCA with PR3 are thought to be instrumental in the pathogenesis of the disease (*24, 25*). However, the conformational epitopes that are recognized by ANCA have not been identified yet (*26*). Since variable glycosylation of antigens may heighten their immunogenicity (*27*), the characterization of structural requirements for the binding of ANCA and the resulting effects on PR3 function are relevant for understanding the pathogenesis of Wegener's granulomatosis.

Asn-linked glycosylation of proteins critically affects their conformational stability and folding, their

*To whom Correspondence should be addressed: Tel: 507 284 2301, Fax: 507 284 4521, E-mail: specks.ulrich@mayo.edu

resistance to digestion by proteases, their intracellular transport, and their interaction with cell-surfaces, extracellular matrix proteins and other ligands, as well as their recognition by the immune system (*27–29*). PR3 contains two potential Asn-linked glycosylation sites, Asn-102 (Asn-Leu-Ser) and Asn-147 (Asn-Val-Thr) (*30*). Sequence alignment indicates that the glycosylation site at Asn-147 is conserved in human elastase and azurocidin as well as in the murine homologues of PR3 and elastase (*2, 31*), whereas the glycosylation site at Asn-102 is shifted C-terminally by four positions in human PR3 and azurocidin compared to human and murine elastase and murine PR3. In contrast to native human elastase (*32*), crystallography of recombinant PR3 (rPR3) expressed in Sf9 insect cells only identified electron densities consistent with Asn-linked glycan moieties at the Asn-147 residue, but not at Asn-102 (*33*). However, glycosylation of recombinant proteins by insect cells differs from mammalian cells (*34, 35*). Hence, for human neutrophil PR3, it remains unknown whether both Asn-glycosylation sites or only Asn-147 are occupied, and moreover, whether occupancy of these sites has functional relevance. The aim of our investigation was to determine whether the two potential Asn-linked glycosylation sites are occupied in human neutrophil PR3, and to evaluate the consequences of site occupancy on enzymatic function, intracellular processing, targeting to granules, and recognition by ANCA.

EXPERIMENTAL PROCEDURES

Materials—Unless indicated otherwise, all materials were purchased from Sigma (St Louis, MO). Purified neutrophil PR3 was purchased from Athens Research & Technology (Athens, GA) and pepsin from Roche Diagnostics (Indianapolis, IN). The monoclonal antibody (moAB) MCPR3-2 and the polyclonal rabbit antibody anti-PR3 were raised against rPR3 expressed in HMC-1 cells as previously described (*36*). The moAB WGM2 was kindly provided by Dr. E. Csernok and Prof. W. L. Gross (Bad Bramstedt, Germany) (*1*), the moABs 4A3, 4A5 and 6A6 by Prof. J. Wieslander (Lund, Sweden) (*37*), and the moABs 12.8, PR3G-2, PR3-G3, PR3-G4, PR3-G6 by Prof. C. G. M. Kallenberg (Groningen, The Netherlands) (*38*). The human mast cell line HMC-1 was a kind gift from Dr. J. H. Butterfield (*39*). PR3-ANCA positive patient sera were obtained from the Clinical Immunology Laboratory, Mayo Clinic, Rochester, MN. No patient identifiers or clinical data about these patients were available to the investigators.

Construction of Vectors and Cell Transfection—The original cDNA insert of rPR3-wt (nucleotide positions 9 to 790 of the published sequence (*30*)) was prepared as described elsewhere (*40*). The glycosylation variants rPR3-N102Q/N147Q, rPR3-N102Q and rPR3-N147Q were prepared using the splicing by overlap extension method (*41*); the primers used are presented in Table 1. To generate the cDNA construct for rPR3-N102Q, overlapping DNA fragments were prepared by PCR using primers 13 and 4, and 14 and 3; with wild-type PR3 cDNA used as template. The resulting DNA fragments were spliced together and cloned into the expression vector pRcCMV^{TM} (Invitrogen). Similarly, to generate rPR3-N147Q, wild-type PR3 cDNA was used as template with primers 15 and 4, and 16 and 3. Finally, for rPR3-N102Q/N147Q, the cDNA construct rPR3-N102Q was used as template with primers 15 and 4 and the primers 16 and 3.

HMC-1 cells were transfected by electroporation as described elsewhere (*40*). Stably transfected cell clones selected in the presence of 600 μg/ml of G418 were screened for rPR3 expression by indirect immunofluorescence using the polyclonal rabbit antibody anti-PR3 and the moAB MCPR3-2 (*42*).

Immunological Methods, Metabolic Labeling and Radiosequencing—Indirect immunofluorescence confocal microscopy was performed using ethanol fixed cytospin preparations (*42*). Immunoblotting was performed as previously described (*36*). Quantitative rPR3 measurements were performed with a capture ELISA using cell-lysates as target antigens. The moAB MCPR3-2 was used as capturing antibody, and the polyclonal rabbit antibody anti-PR3 as detecting antibody as previously described (*36*). This assay was also used to determine ANCA-reactivity with the rPR3 glycosylation variants. To adjust for the previously reported interassay coefficient of variation of about 31% (*36*), positive and negative standard control sera were included on each microtiter plate, and each data point was normalized to the positive reference serum.

A modified cyto-ELISA was used for semiquantitative measurement of intracellular rPR3 in HMC-1 cells expressing rPR3 wt and rPR3 glycosylation variants (*36*). For this assay, 100 000 cells/well were suspended in 96 well microtiter plates; this cell density was chosen to assure that all readings fell within the linear range of the assay, and moAB WGM2 was used for PR3 detection. Irrelevant monoclonal IgG1 was used as negative control.

Immunoprecipitation of rPR3 variants from cell lysates or cell culture supernatants were performed using anti-PR3 moAB MCPR3-2 following previously described protocols (*36, 40, 43*). Pulse-chase experiments and radiosequencing were performed as previously described (*43*).

Table 1. **Primers used for the preparation of the cDNA constructs coding for rPR3-N102Q/N147Q, rPR3-N102Q, and rPR3-N147Q.**

3,	5′-GTC AAA GCT TCC CAC CAT GGC TCA CCG GCC CCC CAG CCC TG-3′
4,	5′-GTA CTC TAG ACG GCC AGC GCT GTG GGA G-3′
13,	5′-CTG AGC AGC CCA GCC CAA CTC AGT GCC TCC GTC-3′
14,	5′-GAC GGA GGC ACT GAG TTG GGC TGG GCT GCT CAG-3′
15,	5′-GTC CTG CAG GAG CTC CAG GTC ACC GTG GTC ACC-3′
16,	5′-GGT GAC CAC GGT GAC CTG GAG CTC CTG CAG GAC-3′

Underlined nucleotides convey the mutation Asn-102 to Gln-102 and Asn-147 to Gln-147.

Deglycosylation of rPR3 Immunoprecipitates and Purified PMN-PR3—Immunoprecipitates of culture supernatants or lysates from metabolically labelled cells were deglycosilated using N-glycosidase F (Boehringer, Mannheim, Germany) as described before (*43*).

Generation, Isolation and Amino Acid Sequence Analysis of PR3 peptides—For digestion of purified neutrophil PR3, 15 µg of PR3 in 15 µl of 0.05 M MES, 0.7 M NaCl, pH 4.5 was diluted with 100 µl 1 M HCl, and incubated for 30 min at room temperature with 75 µl of 0.005 mg/ml of pepsin (Roche Diagnostics, Indianapolis, IN) in water. The reaction was terminated with 50 µl of 1 M Na_2CO_3, and the digest was immediately subjected to high pressure liquid chromatography (HPLC) analysis.

Reduced and alkylated tryptic peptides were generated by incubating 30 µg of purified neutrophil PR3 in 30 µl 0.05 M MES, 0.7 M NaCl, pH 4.5 diluted with 85 µl 0.1 M NH_4HCO_3, 15µl of 0.1 M aqueous $CaCl_2$, and 100 µl CH_3CN at 37°C for 40 to 90 h in the presence of 70µl of 0.01 mg/ml of TPCK-treated trypsin in water. Digests were dried and reconstituted in 400 µl 6 M guanidinium-HCl in 0.1 M TrisCl, pH 7.5 (reconstitution buffer). Reduction of the disulfide bonds was achieved by incubation with 0.65 M dithiothreitol in reconstituting buffer for 2 h at 37°C. Alkylation of the resulting sulfhydrols was achieved with 8 µl of 1 M iodoacetamide in the same buffer (1 h, 37°C). Peptides were isolated for sequence analysis by HPLC using aqueous TFA (0.07%) to TFA in CH3CN (0.05%) gradients on a 250 × 4.5 mm Jupiter C18 column (Phenomenex) with a flow rate of 0.7 ml/min.

Edman degradation was performed using an Applied Biosystems 470A sequencer followed by HPLC analysis of the resulting phenylthiohydantoin amino acids. Peptic cleavages were typical, predominantly following Asn, Leu, Phe or Val residues. In addition to the expected Arg and Lys cleavages, trypsin digests yielded numerous Ala and Val cleavages, most likely due to PR3 digestion of trypsin-generated peptides.

Enzymatic Activity Assays—Esterase activity was determined by measuring the hydrolysis of the synthetic substrate *N*-methoxysuccinyl-Ala-Ala-Pro-Val-pNA as previously described (*40*).

Fractionation of Cell Content—One million HMC-1 cells expressing rPR3-wt, rPR3-N102Q/N147Q, rPR3-N102Q and rPR3-N147Q were washed in 1 × HBSS, centrifuged at 200*g* for 10 min and resuspended in 10 ml of 100 mM KCl, 3 mM NaCl, 3.5 mM $MgCl_2$, 1 mM ATP $[Na]_2$, 10 mM Hepes, pH 6.8. Cells were disrupted by nitrogen cavitation at 350 psi for 20 min at 4°C. Disrupted cells were centrifuged at 500*g* for 10 min at 4°C. The supernatant was collected, 1 ml of 12.5 mM ethylene glycol bis-2-aminoethylether-N,N′,N″,n′-tetraacetic acid (EGTA) was added, and 3 ml of this mixture was layered over a discontinuous Percoll gradient (3 ml of 1.12 and 1.05 g/ml Percoll each). This gradient was centrifuged at 20 000*g* for 15 min at 4°C, and then 1 ml fractions were collected from the bottom of the tube using a fraction collector.

Electron Microscopy—Purified granule fraction was fixed in Trump's fixative (*44*) and rinsed for 30 min in 3 changes of 0.1 M phosphate buffer, pH 7.2, followed by 1 h in phosphate-buffered 1% OsO_4. After rinsing in three changes of distilled water for 30 min, granules were *en bloc* stained with 2% uranyl acetate for 30 min at 60°C. Afterwards, they were rinsed in three changes of distilled water, dehydrated in progressive concentrations of ethanol and 100% propylene oxide, and embedded in Spurr's resin (*45*). Thin (90 nm) sections were cut on a Reichert Ultracut E ultramicrotome, placed on 200 mesh copper grids and stained with lead citrate. Micrographs were taken on a JEOL 1200 EXII operating at 60 KV.

Statistical Analysis—Results were expressed as means ± SE and analysed by Student's *t*-test for paired samples. Differences were considered statistically significant if P was <0.05 (two-tailed).

RESULTS

Both Potential Asn-linked Glycosylation Sites are Occupied in Native PMN-PR3 and in rPR3 Expressed in HMC-1/PR3 Cells—To determine whether native neutrophil PR3 carries sugar side chains at both sites, we subjected purified PR3 from neutrophil azurophil granules to digestion with pepsin and trypsin, to generate peptides spanning either the region of Asn-102 or Asn-147, individually. Resulting peptides were isolated by HPLC and subjected to amino acid sequence analysis. The observed gaps in HPLC sequence analyses were consistent with N-glycosyl-Asn residues since Edman degradation proceeded through such sites but the resulting anilinothiazolinone was not extracted, and no peak could be identified (*46, 47*). Tables 2 and 3 show the sequence analyses from pepsin digest of PR3. For Asn-102, gaps occurred in cycle 8, 9 and 1 in peak P5 (cleavage at Leu-94), peak P7 (cleavage at Leu-93), and

Table 2. **Sequence analysis of peptides from trypsin digest of PR3.**

	Peptide T9	Peak T25	
Cycle	Cleavage at Ala-101	Cleavage at Arg-21	Cleavage at Ala-135
1	–[a]	Gly (89 pmol)	His (NQ[b])
2	Leu (69 pmol)	Asn (41 pmol)	Asp(121 pmol)
3	Ser (NQ[b])	Pro (152 pmol[c])	Pro (152 pmol[c])
4	Ala (76 pmol)	Gly (43 pmol)	Pro (113 pmol)
5	Ser (NQ[b])	Ser (NQ[b])	Ala (105 pmol)
6	–[e]	His (NQ[b])	Gln (77 pmol)
7		Phe (32 pmol)	Val (72 pmol)
8		CMCys (NQ[b])	Leu (67 pmol)
9		Gly (26 pmol)	Gln (70 pmol)
10		Gly (35 pmol)	Glu (42 pmol)
11		Thr (NQ[b])	Leu (47 pmol)
12		Leu (31 pmol)	–[d]
13		Ile (16 pmol)	Val (40 pmol)
14		His (NQ[b])	Thr (NQ[b])
15		Pro (5 pmol)	Val (14 pmol)
16		Ser (NQ[b])	Val (8 pmol)

[a]Published sequence shows Asn at position 102; no signal observed.
[b]Not quantified; peak retention time was consistent with called amino acid.
[c]Both sequences in peak T25 yield Pro on cycle 3.
[d]Published sequence shows Asn at position 147; no signal observed.
[e]Only 5 cycles were run on peptide T9.

peptide T9 (cleavage at Ala-101), respectively; Edman degradation continued normally in all instances. For Asn-147 (Table 2), the gap occurred in cycle 12 in peak T25 (cleavage at Ala-135); and again, Edman degradation proceeded as expected.

To determine whether both potential Asn-linked glycosylation sites are occupied in rPR3 expressed in HMC-1 cells, we compared the electrophoretic mobility of rPR3-wt to the rPR3 glycosylation variants, rPR3-N102Q/N147Q, rPR3-N102Q, and rPR3-N147Q (Fig. 1). Immunoprecipitation of lysates of labelled HMC-1 cells expressing rPR3-wt and the three rPR3 glycosylation variants revealed that the approximate molecular weight for rPR3-wt was 34-36 kDa, compared to about 32 kDa for both rPR3-N102Q and rPR3-N147Q (Fig. 2). The molecular weight of rPR3-N102Q/N147Q was about 29 kDa, consistent with the expected weight of the

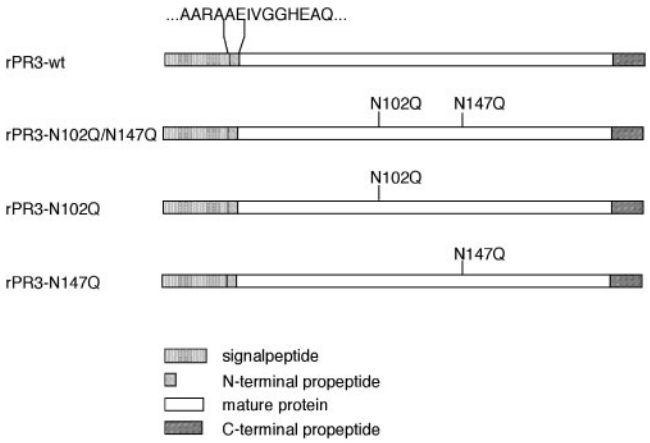

Fig. 1. **Schematic diagram of cDNA constructs.** The construct rPR3-wt codes for the full-length wild-type rPR3 including the signal peptide, the amino-terminal and the carboxy-terminal pro-peptide sequences. The constructs rPR3-N102Q and rPR3-N147Q carry the mutations N102Q and N147Q coding for glutamine instead of the asparagine in position 102 and 147, respectively. The construct rPR3-N102Q/N147Q carries both mutations coding for the rPR3 variant without any Asn-linked sugar moieties. The amino acid numbering system is based on the published sequence (*30*).

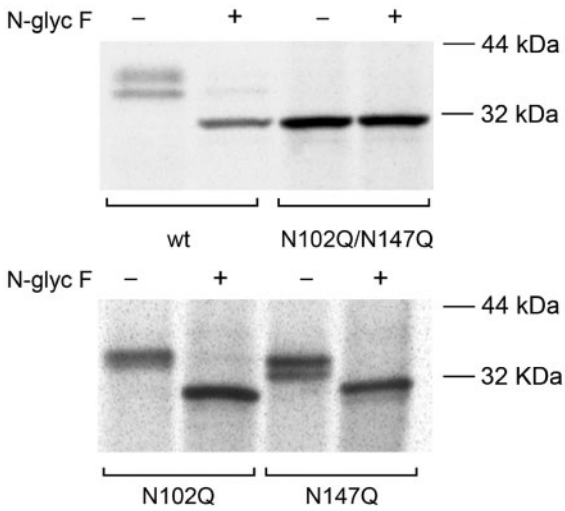

Fig. 2. **Both Asn-linked glycosylation sites of rPR3 expressed in HMC-1 cells are occupied.** Immunoprecipitates of lysates of metabolically labelled HMC-1 cells expressing rPR3-wt, rPR3-N102Q, rPR3-N147Q and rPR3-N102Q/N147Q, were separated by SDS-PAGE (12% gels) under reducing conditions. Prior to immunoprecipitation, the rPR3 variants were treated (+) with N-glycosidase F (N-glyc F) to remove Asn-linked glycans. Control rPR3 variants were exposed to the same digest conditions in the absence (-) of N-glycosidase F. Deglycosylation of rPR3-wt, rPR3-N012Q and rPR3-N147Q resulted in a molecular weight reduction from about 36, 32 and 32 kDa, respectively, to 29 kDa. No change in the molecular weight was detectable for rPR3-N102Q/N147Q. The figure shows a representative example of 3 different experiments.

Table 3. **Sequence analysis of peptides from pepsin digest of PR3.**

	Peak P5		Peak P7	
Cycle	Cleavage at Asn-55	Cleavage at Leu-94	Amino-terminus	Cleavage at Leu-93
1	Val (132 pmol)	Ile (144 pmol)	Ile (206 pmol)	Leu (42 pmol)
2	Val (92 pmol)	Gln (97 pmol)	Val (195 pmol)	Ile (45 pmol)
3	Leu (130 pmol[a])	Leu (130 pmol[a])	Gly (153 pmol)	Gln (29 pmol)
4	Gly (60 pmol)	Ser (NQ[b])	Gly (156 pmol)	Leu (23 pmol)
5	Ala (78 pmol)	Ser (NQ[b])	His (NQ[b])	Ser (NQ[b])
6	His (NQ[b])	Pro (51 pmol)	Glu (105 pmol)	Ser (NQ[b])
7	Asn (34 pmol)	Ala (33 pmol)	Ala (92 pmol)	Pro (21 pmol)
8	Val (42 pmol)	Asn (13 pmol[c])	Gln (72 pmol)	Ala (45 pmol)
9	Arg (NQ[b])	Leu (21 pmol)	Pro (64 pmol)	–[d]
10	Thr (NQ[b])	Ser (NQ[b])	His (NQ[b])	Leu (8 pmol)
11	Gln (15 pmol)	Ala (28 pmol)	–[e]	
12	Glu (31 pmol)	Ser (NQ[b])		
13	Pro (12 pmol)	Val (6 pmol)		

[a]Both sequences in peak P5 yielded Leu on cycle 3.
[b]Not quantified; peak retention time was consistent with called amino acid.
[c]The small Asn signal of cycle 8 is likely due to 'lag' from cycle 7 (Asn-62). If Asn-102 was not glycosylated, the yield on cycle 8 would have been higher than the preceding cycle due to the additive effect of the 'lag' from cycle 7 (Asn-62), and the Asn-102 signal on cycle 8. However, the signal is diminished, indicating no contribution from Asn-102 and thus glycosylation.
[d]Published sequence shows Asn at position 102; no signal observed.
[e]Only 10 cycles were run on Peak P7.

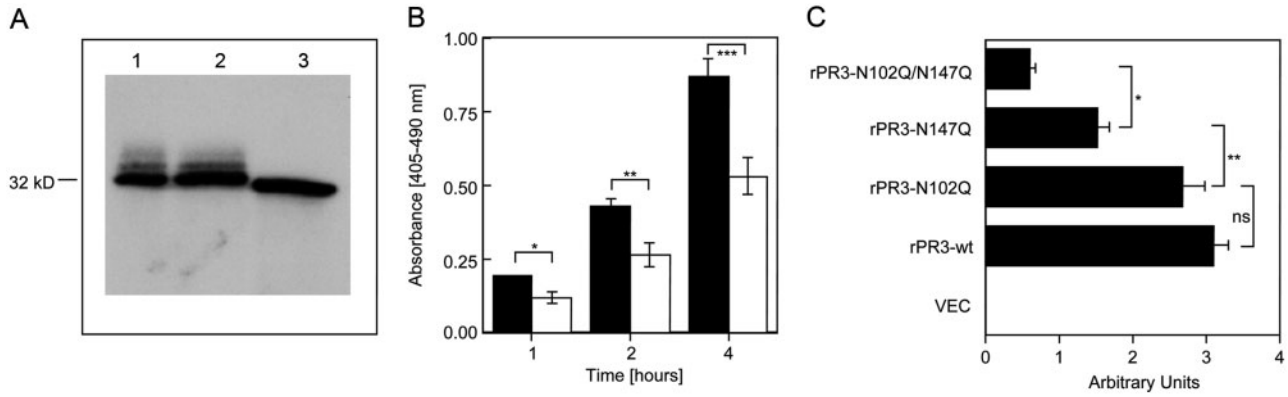

Fig. 3. **Hydrolysis of the substrate *N*-methoxysuccinyl-Ala-Ala-Pro-Val-pNA is affected by the glycosylation status of PR3.** (A) Purified neutrophil PR3 (lane 1) incubated in the absence (lane 2) and presence of N-glycosidase F (lane 3) were separated by SDS-PAGE (12% gel), and the moAB MCPR3-2 was used for detection of PR3. The gel indicates that treatment with N-glycosidase F produced complete removal of Asn-linked glycans, but no proteolytic degradation of PR3. (B) Hydrolysis of the substrate *N*-methoxysuccinyl-Ala-Ala-Pro-Val-pNA by deglycosylated neutrophil PR3 (white bars) is significantly reduced compared to native neutrophil PR3 (black). The plot shows the means ± SE of 4 experiments. $^{*}P = 0.019$; $^{**}P = 0.036$; $^{***}P = 0.043$. (C) Hydrolysis of *N*-methoxysuccinyl-Ala-Ala-Pro-Val-pNA by HMC-1 cells expressing all rPR3 variants, normalized for the total intracellular rPR3 as determined by cyto-ELISA using the moAB WGM2. The enzymatic activity of cells expressing rPR3-N102Q/N147Q was significantly lower than cells expressing rPR3 with at least one preserved Asn-linked glycan, and glycosylation at Asn-147 appears to be critical for optimal enzymatic activity. Each experiment was performed in duplicate. The plot shows the means ± SE of 5 experiments. ($^{*}P = 0.0004$, $^{**}P = 0.002$, ns = not significant). (VEC: HMC1-cells transfected with the empty expression vector).

amino acid backbone (*30*). After digestion with N-glycosidase F, the molecular weight of all rPR3-variants containing Asn-linked glycans was reduced to 29 kDa, while rPR3-N102Q/N147Q remained unchanged (Fig. 2). Both rPR3-wt and rPR3-N147Q ran as double band, which was reduced to a single one after treatment with N-glycosidase F, indicating that glycosylation isoforms were the predominant cause for this electrophoretic pattern.

Together, these data indicate that both potential Asn-linked glycosylation sites of PR3 are occupied with sugar side chains, both in native neutrophil PR3 and in rPR3 expressed in HMC-1 cells. Consequently, this expression system can be used to address the functional role of the individual glycosylation sites.

Removal of Asn-linked Glycans Affects the Hydrolysis of N-methoxysuccinyl-Ala-Ala-Pro-Val-pNA by PR3—First, to determine whether Asn-linked glycosylation is required for enzymatic activity of PR3, we compared the activity of purified neutrophil PR3 versus deglycosylated neutrophil PR3 against the substrate *N*-methoxysuccinyl-Ala-Ala-Pro-Val-pNA. Purified neutrophil PR3 was digested with N-glycosidase F resulting in complete removal of Asn-linked glycans after 18 h (Fig. 3A, lane 3). PR3 subjected to the same reaction conditions but in absence of N-glycosidase F showed no evidence of proteolytic degradation (Fig. 3A, lane 2). Hydrolysis of *N*-methoxysuccinyl-Ala-Ala-Pro-Val-pNA by neutrophil PR3 was reduced by 40% as a result of deglycosylation (Fig. 3B). This indicates that the presence of Asn-linked glycans is not an absolute requirement for hydrolytic activity of PR3 *per se*, but for optimal efficiency.

Second, to determine which of the glycan moieties was more relevant for enzymatic activity, we compared the hydrolysis of *N*-methoxysuccinyl-Ala-Ala-Pro-Val-pNA by cell lysates of HMC-1 cells expressing rPR3-wt and rPR3 glycosylation variants. Since different cell clones express different amount of rPR3, the measured enzymatic activity is presented in relation to the immunologically detectable total intracellular rPR3 as determined by cyto-ELISA. Fig. 3C shows that the overall hydrolytic activity of cells expressing rPR3-N102Q/N147Q was significantly reduced in comparison to rPR3-N147Q, rPR3-N102Q and rPR3-wt, with no significant difference between the later two. Additionally, glycosylation at Asn-147 is required for optimal hydrolytic activity of rPR3, whereas glycosylation at Asn-102 is not.

The observed reduction in hydrolytic activity of rPR3-N102Q/N147Q in relation to rPR3-wt was more pronounced than the reduction induced by deglycosylation of purified neutrophil PR3 (Fig. 3B and C). Several factors might be responsible for this difference. Modifications of the amino acid backbone induced by the Asn to Gln mutation might possibly have additional conformational effects, which may render these rPR3 variants more susceptible to intracellular proteolytic degradation, or may negatively affect substrate binding and cleavage. Furthermore, altered kinetics of intracellular processing from proenzyme to mature enzyme could contribute to the observed effects.

The Carbohydrate Chain at Asn-147 Appears Critical for Thermostability of PR3—As thermostability of PR3 and consequently its resistance to intracellular proteolytic degradation might be affected by the glycosylation status, we evaluated the thermostability of deglycosylated neutrophil PR3 and rPR3 glycosylation variants. When deglycosylated neutrophil PR3 was incubated at 57°C, the hydrolysis of N-methoxysuccinyl-Ala-Ala-Pro-Val-pNA was reduced in a time-dependent fashion (Fig. 4A). To determine which of the sugar moieties was required for thermostability, we measured the hydrolysis of N-methoxysuccinyl-Ala-Ala-Pro-Val-pNA

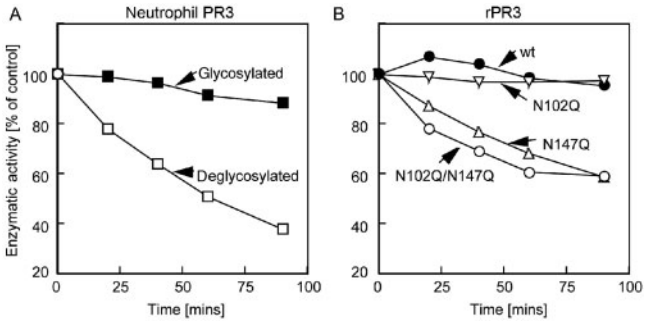

Fig. 4. **Thermal stability of PR3 is affected by the glycosylation status.** (A) Asn-linked glycosylation conveys thermostability of purified neutrophil PR3. Purified neutrophil PR3 was incubated in the presence and absence of N-glycosidase F. The hydrolysis of the substrate *N*-methoxysuccinyl-Ala-Ala-Pro-Val-pNA by the resulting deglycosylated neutrophil PR3 (white squares) and control neutrophil PR3 (black squares) was determined for the indicated time periods. (B) Similarly, hydrolysis of *N*-methoxysuccinyl-Ala-Ala-Pro-Val-pNA by lysates of HMC-1 cells expressing rPR3-wt, rPR3-rPR3-N102Q/N147Q, rPR3- N102Q, and rPR3-N147Q was measured. Thermostability of rPR3-wt and neutrophil PR3 was equivalent, and glycosylation at Asn-147 appears sufficient to preserve it. The figures show representative examples of three experiments, and each experiment was performed in triplicate.

by lysates of HMC-1 cells expressing rPR3-wt, rPR3-N102Q, rPR3-N147Q and rPR3-N102Q/N147Q which had been incubated at 57°C for various time periods. Glycosylation at Asn-147 appears sufficient to preserve thermostability of PR3 (Fig. 4B).

The Carbohydrate Chain at Asn-102 Appears Critical for Efficient N-terminal Processing of PR3—As previously shown (Fig. 3), all three rPR3 glycosylation variants expressed in HMC-1 cells have enzymatic activity, implying that they all are amino-terminally processed. Since glycosylation status might affect the efficiency of amino-terminal processing and thereby contribute to the reduced relative enzymatic activity of rPR3-N102Q/N147Q, pulse chase experiments and subsequent amino-terminal radiosequencing of cell lysates and cell media were performed. Immunoprecipitates of cell media supernatants from all glycosylation variants, obtained at 3, 6 and 24 h of chase, displayed isoleucine in the third position (data not shown), indicating that only N-terminally unprocessed rPR3 is secreted into the media.

Radiosequencing of immunoprecipitates of pulse-labelled cell lysates indicates that N-terminal proteolytic processing of rPR3-N102Q/N147Q is delayed compared to rPR3-wt and remains incomplete after 6 h of chase (Fig. 5, Table 4). The N-terminal processing of rPR3-N102Q was similarly delayed, whereas rPR3-N147Q was processed like rPR3-wt. After 24 h of chase, immunoprecipitates of cell lysates of all rPR3 glycosylation variants displayed the [^{3}H]-isoleucine peak in the first position like rPR3-wt (data not shown). These data suggest that glycosylation at Asn-102 is a critical determinant of efficient N-terminal processing, whereas glycosylation at Asn-147 is less relevant in this context.

Effect of Asn-linked Glycosylation on Secretion and Targeting to Granules of rPR3—We further investigated the effects of differential glycosylation on the secretion of the unprocessed pro-form of rPR3 into the media supernatants. Pulse chase experiments indicated that secretion of the pro-form of all three rPR3 glycosylation variants into media supernatants is not dependent on the presence of Asn-linked sugars (Fig. 6A). On the contrary, the relative proportion of rPR3-N102Q/N147Q secreted into media supernatants was about double than rPR3-wt (Fig. 6B).

The structural requirements for packaging of PR3 into neutrophil granules remain unknown. To determine whether glycosylation status of rPR3 affects its targeting to HMC-1 cell granules, we performed indirect immunofluorescence confocal microscopy on ethanol-fixed cytospin preparations of HMC-1 cells expressing rPR3-wt and rPR3 glycosylation variants, using the moAB WGM2. This antibody binds preferentially to fully processed conformationally intact PR3 (*1*). As seen in Fig. 7, the granular cytoplasmic immunofluorescence pattern of cells expressing the different rPR3 glycosylation variants was indistinguishable from those expressing rPR3-wt.

Furthermore, using a discontinuous Percoll gradient (*48*), granules were isolated from HMC-1 cells transfected with the empty expression vector, and from HMC-1 cells expressing all rPR3 glycosylation variants. Electron microscopy confirmed that the visible upper band collected in fractions #5 and #6 contained HMC-1 cell granules (Fig. 8A, B). Figure 8C, shows an electron microscopy image of HMC-1 cell and Fig. 8D a close-up of cytoplasmic granules for comparison. Hydrolysis of the substrate *N*-methoxysuccinyl-Ala-Ala-Pro-Val-pNA was performed with aliquots of each gradient fraction. The majority of hydrolytic activity of all four rPR3 expressing cell types was localized in the granule-containing fractions (Fig. 8E). The granule fraction of HMC-1 cells transfected with the empty expression vector had minimal hydrolytic activity (<2% compared to rPR3-wt expressing cells). These observations indicate that Asn-linked glycosylation is not a requirement for targeting of PR3 to granules.

Effects of Asn-linked Glycosylation of rPR3 on Recognition by Anti-PR3 moABs and ANCA—PR3 is the primary target antigen for ANCA in patients with Wegener's granulomatosis. Patients with this form of autoimmune vasculitis have ANCA, which recognize different, undefined conformational epitopes of PR3. Several moABs that recognize essentially four clusters of epitopes against PR3 have been developed (*38*). To determine whether any of the Asn-linked glycans contribute significantly to these epitopes and their recognition by the moABs, we performed indirect immunofluorescence on HMC-1 cells expressing rPR3-wt, and rPR3 glycosylation variants. Two representative moABs for each of the four major epitopes were used for detection of the rPR3 variants. All moABs tested recognized all the glycosylation variants equally (data not shown), indicating that that none of the major PR3 epitopes, which are distinguishable by currently available moABs, is defined or significantly affected by the glycosylation status of PR3.

To determine whether any of the Asn-linked glycans were essential for the recognition of PR3 by ANCA, we tested 40 ANCA positive serum samples of individual

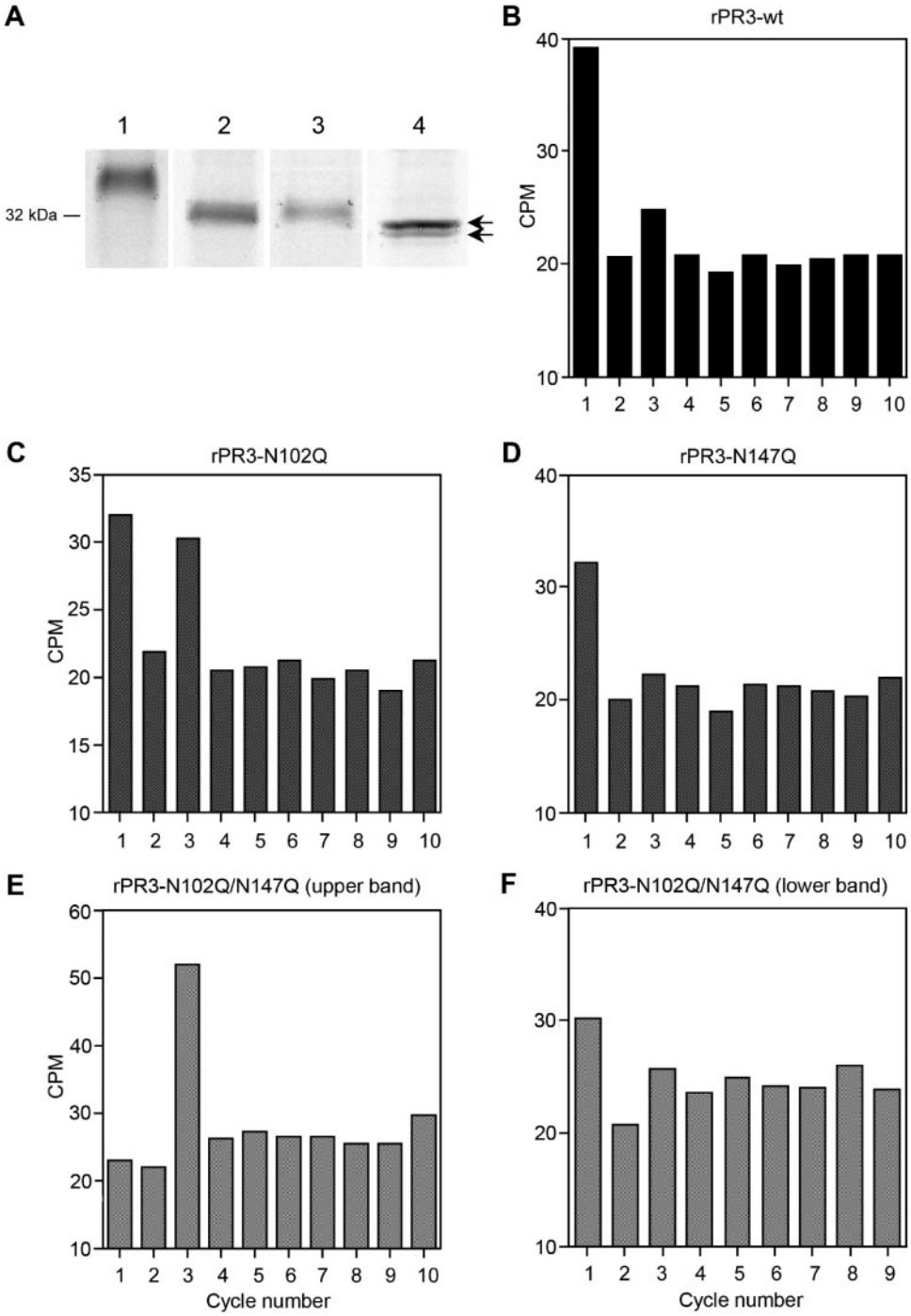

Fig. 5. **Glycosylation at Asn-102 is required for efficient N-terminal processing of rPR3.** Proteins of HMC-1 cells expressing rPR3-wt, rPR3-N102Q, rPR3-N147Q and rPR3-N102Q/N147Q were biosynthetically pulse labelled with ^{3}H-isoleucine for 30 min. After 3, 6 and 24 h of incubation with unlabelled media (chase), cells and media supernatants were collected. The labelled proteins were immunoprecipitated with the polyclonal rabbit anti-PR3 antibody, separated by SDS-PAGE (12% gel) and transferred to a PVDF-membrane. PR3-specific bands were identified by contact autoradiography, cut out of the filter, and sequenced by Edman degradation followed by scintillation counting of radioactivity associated with each cycle. (A) Autoradiograms of rPR3-wt (*1*), rPR3-N102Q (*2*), rPR3-N147Q (*3*) and rPR3- N102Q/N147Q (*4*) were used to identify their position on the PVDF membrane. The arrows indicate the upper and lower bands for the migration of rPR3-N102Q/N147Q. The radiosequencing results for the immunoprecipitates of cell lysates after 3 h of chase are shown (B to F). The 3-h immunoprecipitation band of rPR3-N102Q displayed ^{3}H-isoleucine activity in the first and third position (C). In contrast, rPR3-wt (B) and rPR3-N147Q (D) displayed most of the ^{3}H-isoleucine activity in the first position. For rPR3-N102Q/N147Q each band (A, lane 4) was sequenced separately. The upper (E) and lower (F) bands represent N-terminally unprocessed and processed rPR3-N102Q/N147Q, respectively. All pulse-chase experiments and radiosequencing analyses shown were performed at least twice. CPM (counts per minute).

Table 4. **Summary of radiosequencing results.**

N-glycosylation variant	Time of chase (h)	Electrophoretic band analysed	Cycle # of [^{3}H]-Isoleucine peak
rPR3-wt	3	single	1
	6	single	1
rPR3-N102Q/ N147Q	3	upper of doublet	3
	3	lower of doublet	1
	6	upper of doublet	3
	6	lower of doublet	1
rPR3-N102Q	3	single	1 & 3
	6	single	1 & 3
rPR3-N147Q	3	single	1
	6	single	1

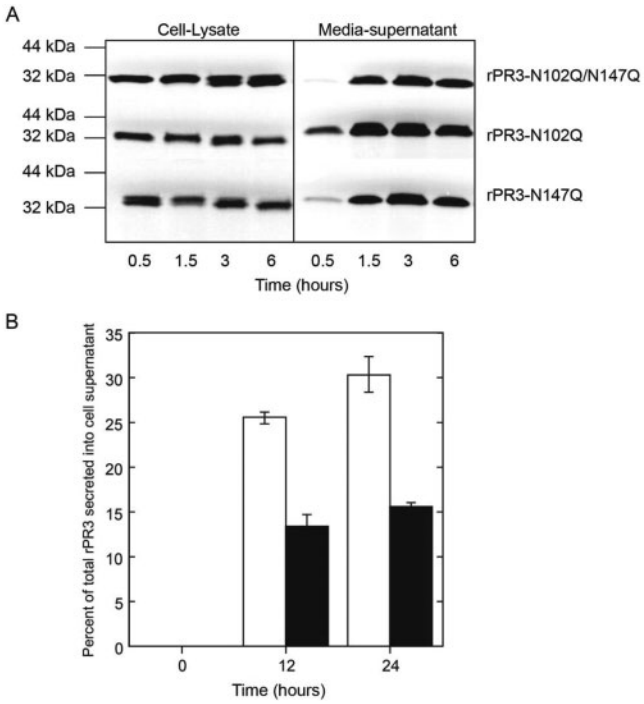

Fig. 6. **Asn-linked glycosylation is not required for secretion of pro-PR3 into media supernatants.** (A) Pulse-chase experiments indicate that all three rPR3 glycosylation variants are secreted into the cell culture supernatants. Ten million pulse-labelled cells per time point were lysed at the indicated time intervals of chase (hours), and subjected to immunoprecipitation using the rabbit polyclonal anti-PR3 antibody, SDS-PAGE (12% gel, under reducing conditions) and autoradiography. Similarly, media supernatants were collected at the indicated time points of chase and subjected to immunoprecipitation. (B) A larger proportion of total rPR3-N102Q/147Q (white bars) is secreted into the cell supernatant compared to rPR3-wt (black bars). At time 0, fresh cell culture media, shown to have no PR3, was used to resuspend washed cells. Cells and media were collected at 12 and 24 h of incubation, and PR3 content was determined quantitatively by capture ELISA for cell lysates and media supernatants. Results were normalized for cell numbers and expressed as proportion of total PR3 measured. The figure shows the means ± SE of three separate experiments.

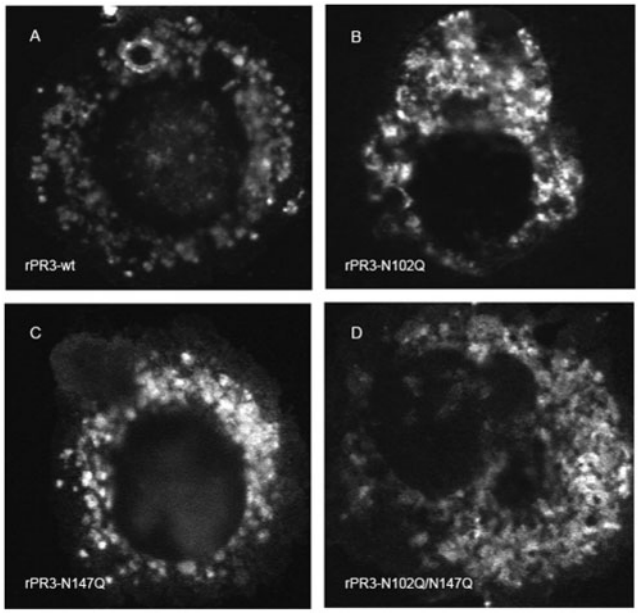

Fig. 7. **Effect of glycosylation status on targeting to granules.** Indirect immunofluorescence of cytospin preparations of ethanol-fixed HMC-1 cells expressing rPR3-wt (A), rPR3-N102Q (B), rPR3-N147Q (C) and rPR3- N102Q/N147Q (D). The moAB WGM2 was used for detection of rPR3 variants. All four glycosylation variants appear enriched in granular structures.

patients suffering from Wegener's granulomatosis in parallel by capture ELISA (*36*). Cell lysates of HMC-1 cells expressing the four recombinant glycosylation variants were used as target antigens. The affinity of MCPR3-2 for the four different target antigens was equivalent as documented by parallel antigen dilution curves (data not shown). All 40 ANCA positive sera reacted with all four glycosylation variants, but in 8 of the 40 (20%), there were clear differences in the optical density generated by the binding of ANCA to the glycosylation variants. In four sera, the optical density with rPR3-N147Q was significantly enhanced compared to the other three glycosylation variants (Fig. 9A). In other four sera, the optical density with rPR3-N102Q/ N147Q was significantly reduced compared to rPR3-wt, rPR3-N102Q or rPR3-N147Q (Fig. 9B). Altogether, these data indicate that neither of the two Asn-linked glycans is a major requirement for recognition of PR3 by anti-PR3 moABs or ANCA. However, the absence of the glycan at position Asn-147 may enhance the accessibility of an epitope recognized by a defined subset of ANCA.

DISCUSSION

This study was designed to determine whether the two potential Asn-linked glycosylation sites are occupied in human neutrophil PR3, and to evaluate the consequences of site occupancy on enzymatic function, intracellular processing, targeting to granules, and recognition by ANCA. Our findings demonstrate that glycosylation occurs at both sites in neutrophil PR3 as well as rPR3 expressed in HMC-1 cells, and the extent of glycosylation at Asn-102 and Asn-147 is similar, but their functional

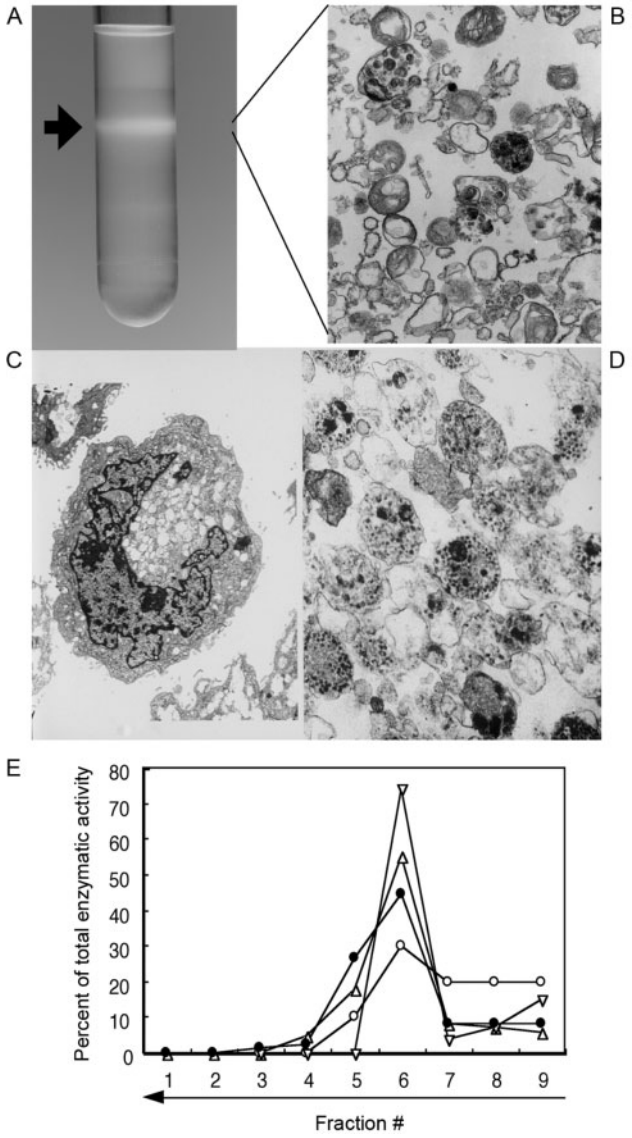

Fig. 8. **Enzymatic activity of glycosylated rPR3 is concentrated in the granule fraction of HMC-1 cell lysates.** (A) Postnuclear cavitate of HMC-1 cells after centrifugation on a discontinuous Percoll gradient. The most prominent visible band at the interface (arrow) contains mostly granules and was collected (fractions # 5 and # 6 starting from the bottom of the gradient). (B) Electron microscopy of fraction # 6 showed that it contains mostly HMC-1 cell granules. (C) Electron microscopy image of HMC-1 cell and (D) close-up of cytoplasmic granules. (E) The hydrolysis of the substrate *N*-methoxysuccinyl-Ala-Ala-Pro-Val-pNA by each gradient fraction (equal volume aliquots were used) was measured. Shown is the proportion (%) of total hydrolytic activity in each gradient fraction for rPR3-wt (black circles), rPR3-N102Q (inverted triangles), rPR3-N147Q (triangles) and rPR3-N102Q/N147Q (white circles). The plot shows a representative example of three separate experiments performed for each rPR3 glycosylation variant. The absolute optical densities (405–490 nm) of the peak fractions from the shown experiment were 2.7 for rPR3-wt, 1.0 for rPR3-N102Q, 2.3 for rPR3-N147Q, and 0.15 for rPR3-N102Q/N147Q. The maximal optical density of any fraction obtained from HMC-1 cells transfected with the empty expression vector was 0.03 (data not shown). The arrow indicates the direction of sedimentation.

significance is not. Although glycosylated and deglycosylated neutrophil PR3 and rPR3 glycosylation variants have enzymatic activity, glycosylation of Asn-147 is required for optimal hydrolytic activity. Moreover, glycosylation of Asn-147 seems to be critical for thermostability of PR3. We also found that glycosylation is not an absolute requirement for amino-terminal processing of rPR3 or for targeting to HMC-1 cell granules. However, glycosylation of Asn-102 appears to be important for efficient N-terminal processing of PR3.

We have shown that optimal enzymatic activity and thermostability of PR3 depend on the glycosylation at Asn-147, but not at Asn-102. This suggests that glycosylation at Asn-147 is crucial for the conformational stability of PR3. Since thermostability of rPR3-N102Q/N147Q, rPR3-N147Q and deglycosylated neutrophil PR3 was similar, the observed decrease in their enzymatic activity cannot be attributed to alterations of the amino acid backbone, produced by the substitution of Asn- to Gln-residues, but to the presence or absence of sugar side chains at Asn-147.

We further investigated the effects of differential glycosylation of PR3 on intracellular processing, secretion, and targeting to granules. It has been demonstrated that the amino-terminally unprocessed pro-form of PR3, carrying untrimmed high-mannose glycans, is secreted by U937 cells producing endogenous PR3, by hematopoietic cells, and by epithelial 293 cells expressing rPR3 (*40, 43, 49, 50*). Treatment of U937 cells with tunicamycin, which blocks the Asn-linked core glycosylation, does not seem to prevent granule targeting or amino-terminal processing (*49*). However, it has been reported to abolish secretion of PR3 into the media supernatant (*49*). We therefore hypothesized that glycosylation may be required for secretion of the pro-form of PR3 via the unregulated pathway. Our data indicate that the amino-terminally unprocessed pro-form of PR3 was secreted into the media supernatants. In fact, a higher proportion of the glycan-deficient rPR3 (rPR3-N102Q/N147Q) was secreted via the non-regulated pathway into the media supernatant compared to rPR3-wt or rPR3 carrying at least one Asn-linked glycan. Most likely, this discrepancy is due to the global result of tunicamycin on Asn-linked glycosylation of any newly synthesized cellular protein, which causes several additional effects on cellular functions. Some of these effects may disturb the secretion of PR3. In contrast, the use of *in vitro* mutagenesis is a more selective intervention that allows the assessment of Asn-linked glycosylation of rPR3 as a single variable. Our findings, clearly demonstrate that Asn-linked glycosylation of rPR3 is not required for secretion via the non-regulated pathway.

We also found that cleavage of the amino-terminal activation dipeptide occurred in the absence of Asn-linked glycans, and Asn-linked glycosylation did not seem to be required for targeting of amino-terminally processed rPR3 to granules. These findings are consistent with observations made in U937 cells treated with tunicamycin, where inhibition of glycosylation did not prevent the shift of isoleucine from the third to the first position (implying the removal of the amino-terminal activation dipeptide) in pulse-chase experiments (*49*). Similarly, glycosylation of cathepsin G was found not to be essential for enzymatic activation or granule sorting

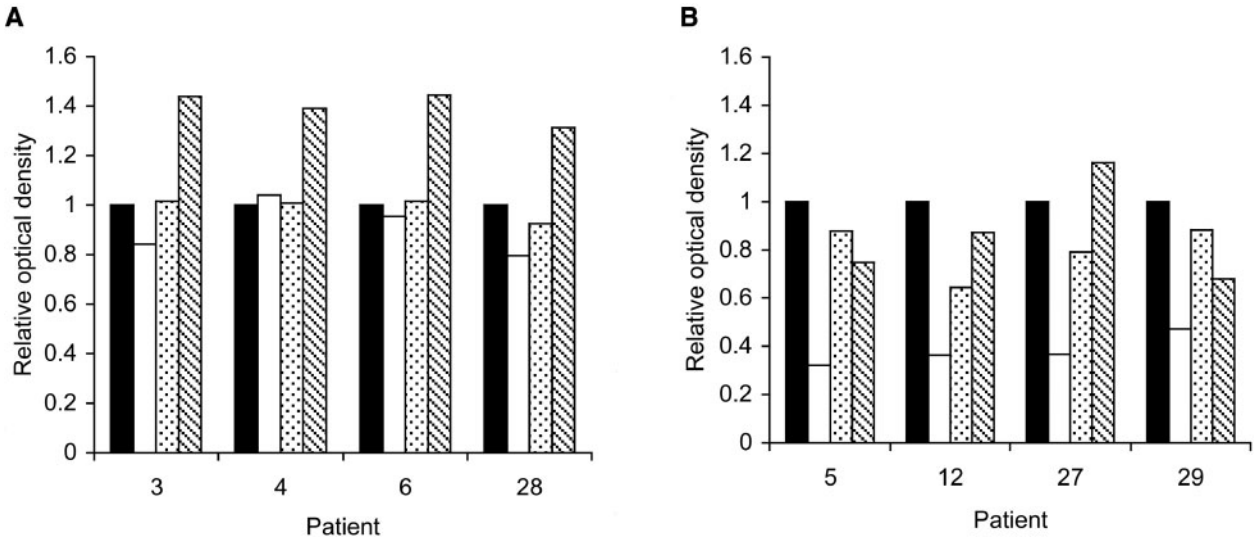

Fig. 9. **Recognition of rPR3 glycosylation variants by ANCA.** Cell lysates of HMC-1 cells expressing rPR3-wt (black bars), rPR3-N102Q/N147Q (white bars), rPR3-N102Q (dotted bars) and rPR3-N147Q (hatched bars) were used as target antigens in the capture ELISA with the moAB MCPR3-2 as capturing antibody (36). Panel A shows the optical densities obtained in the four patients that displayed increased reactivity with rPR3-N147Q (patients 3, 4, 6 and 28). Panel B shows the four patients with reduced reactivity with rPR3-N102Q/N147Q (patients 5, 12, 27 and 29). For each patient, the ANCA reactivity with each glycosylation variant was normalized to the reactivity with rPR3-wt.

in the rat basophilic/mast cell line RBL and in the murine myeloblast-like cell line 32D (*51*). However, it remained unclear whether the efficiency of these processes was affected by the Asn-glycan of cathepsin G. Our studies, using *in vitro* mutagenesis applied to each Asn-glycosylation site individually and in combination, revealed that glycosylation at Asn-102, but not at Asn-147, appears to be critical for the efficiency of amino-terminal processing of rPR3.

Over the last decade PR3 has become the subject of intense investigation focusing on its role as the principal target antigen for ANCA in patients with Wegener's granulomatosis. ANCA recognize conformational epitopes (*26*). Since the addition and appropriate trimming of Asn-linked glycans facilitates the formation of the tertiary structure of many proteins, and misfolded proteins are subject to intracellular degradation (*28, 29*), and Asn-linked glycosylation contributes to the stability of the PR3 molecule, it could be expected that glycosylation of PR3 will affect its recognition by ANCA. To date, the significance of the glycosylation status of PR3 for ANCA recognition has not been investigated in detail. Witko-Sarsat et al. analysed five sera from patients with Wegener's granulomatosis by Western blot, using glycosylated and deglycosylated neutrophil PR3 as target antigen; no difference in ANCA binding was found between the two antigen preparations (*52*). In the present study, we performed a more detailed analysis using 40 random serum samples from patients with Wegener's granulomatosis, with a variety of ANCA titres. Our results obtained with a capture ELISA system, in which the conformation of the target antigen is preserved, confirmed that glycosylation is not an absolute requirement for ANCA recognition. Thus, the conformational epitopes recognized by ANCA seem to be largely defined by the disulfide bonds, and to a more significant extent by the conformational changes associated with the cleavage of the amino-terminal activation dipeptide (*26, 43, 52, 53*). Nevertheless, we found that 20% of the serum samples from patients with Wegener's granulomatosis showed significant differences in the binding of ANCA to the glycosylation variants. These data provide further evidence for the heterogeneity of ANCA response. A subset of ANCA displayed increased binding to rPR3-N147Q, suggesting reactivity with an epitope that is rendered more accessible in the absence of a glycan at Asn-147. Another subset of ANCA showed reduced binding to the rPR3 glycosylation variant lacking N-glycans altogether, suggesting that this subset is particularly sensitive to minimal changes in the conformation of PR3 that is conveyed by the presence of at least one intact Asn-linked glycan.

The glycosylation status of autoantigens may be of importance for the pathogenesis of some autoimmune diseases. Aberrant glycosylation may render target antigens more immunogenic by exposing cryptic epitopes (*54*). Deglycosylated antigens may be more susceptible to proteases, involved in the generation of autoantigenic protein fragments (*55, 56*). Conversely, for some autoimmune diseases glycosylation of the target antigen seems to be a requirement for its antigenicity (*57–59*). Therefore, a more detailed analysis of the clinical significance of ANCA recognition of the glycosylation variants of PR3, using sera from a large well-defined prospective study of patients with Wegener's granulomatosis has been initiated.

In conclusion, the present study demonstrates that glycosylation occurs at both sites in neutrophil PR3 as well as rPR3 expressed in HMC-1 cells, and the extent of glycosylation at Asn-102 and Asn-147 is similar,

but their functional significance is not. Glycosylated and deglycosylated neutrophil PR3 and rPR3 glycosylation variants have enzymatic activity, but glycosylation of Asn-147 is required for optimal hydrolytic activity, and in addition it seems critical for thermostability of PR3. Glycosylation is not an absolute requirement for amino-terminal processing of rPR3 or for targeting to cell granules, but glycosylation of Asn-102 appears to be important for efficient N-terminal processing of PR3. Finally, in 20% of the patients with Wegener's granulomatosis, epitope recognition by ANCA seems to be affected by the glycosylation status of PR3.

This study was supported in part by grants AHA 96008260 from the American Heart Association, and R21-AI47572 and R01-AR49806 from the National Institutes of Health (to U.S.) and by funds from the Mayo Foundation. We thank Jon E. Charlesworth for helping with electron microscopy, James E. Tarara for assistance with confocal microscopy, and Hua Tang for performing the thermostability experiments.

REFERENCES

1. Csernok, E., Ludemann, J., Gross, W.L., and Bainton, D.F. (1990) Ultrastructural localization of proteinase 3, the target antigen of anti-cytoplasmic antibodies circulating in Wegener's granulomatosis. *Am. J. Pathol.* **137**, 1113–1120
2. Zimmer, M., Medcalf, R.L., Fink, T.M., Mattmann, C., Lichter, P., and Jenne, D.E. (1992) Three human elastase-like genes coordinately expressed in the myelomonocyte lineage are organized as a single genetic locus on 19pter. *Proc. Natl. Acad. Sci. USA.* **89**, 8215–8219
3. Sturrock, A.B., Franklin, K.F., Rao, G., Marshall, B.C., Rebentisch, M. B., Lemons, R. S., and Hoidal, J. R. (1992) Structure, chromosomal assignement, and expression of the gene for proteinase-3. *J. Biol. Chem.* **29**, 21193–21199
4. Rao, N.V., Wehner, N.G., Marshall, B.C., Gray, W.R., Gray, B.H., and Hoidal, J.R. (1991) Characterization of proteinase-3 (PR-3), a neutrophil serine proteinase. *J. Biol. Chem.* **266**, 9540–9548
5. Halbwachs-Mecarelli, L., Bessou, G., Lesavre, P., Lopez, S., and Witko-Sarsat, V. (1995) Bimodal distribution of proteinase 3 (PR3) surface expression reflects a constitutive heterogeneity in the polymorphonuclear neutrophil pool. *FEBS.* **374**, 29–33
6. Csernok, E., Ernst, M., Schmitt, W., Bainton, D.F., and Gross, W.L. (1994) Activated neutrophils express proteinase 3 on their plasma membrane *in vitro* and *in vivo*. *Clin. Exp. Immunol.* **95**, 244–250
7. Renesto, P., Halbsachs-Mecarelli, L., Nusbaum, P., Lesavre, P., and Chignard, M. (1994) Proteinase 3. A neutrophil proteinase with activity on platelets. *J. Immunol.* **152**, 4612–4617
8. Renesto, P., Si-Tahar, M., Moniatte, M., Balloy, V., Van Dorsselaer, A., Pidard, D., and Chignard, M. (1997) Specific inhibition of thrombin-induced cell activation by the neutrophil proteinases elastase, cathepsin G, and proteinase 3: evidence for distinct cleavage sites within the amino-terminal domain of the thrombin receptor. *Blood* **89**, 1944–1953
9. Leid, R.W., Ballieux, B.E. P.B., van der Heijden, I., Kleyburg-van der Keur, C., Hagen, E.C., van der Woude, F.J., and Daha, M.R. (1993) Cleavage and inactivation of human C1 inhibitor by the human leukocyte proteinase, proteinase 3. *Eur. J. Immunol.* **23**, 2939–2944
10. Padrines, M., Wolf, M., Walz, A., and Baggiolini, M. (1994) Interleukin-8 processing by neutrophil elastase, cathepsin G and proteinase-3. *FEBS Lett.* **352**, 231–235
11. Robache-Gallea, S., Morand, V., Bruneau, J.M., Schoot, B., Tagat, E., Réalo, E., Chouaib, S., and Roman-Roman, S. (1995) In vitro processing of human tumor necrosis factor-α. *J. Biol. Chem.* **270**, 23688–23692
12. Coeshott, C., Ohnemus, C., Pilyavskaya, A., Ross, S., Wieczorek, M., Kroona, H., Leimer, A.H., and Cheronis, J. (1999) Converting enzyme-independent release of tumor necrosis factor alpha and IL-1beta from a stimulated human monocytic cell line in the presence of activated neutrophils or purified proteinase 3. *Proc. Natl. Acad. Sci. USA.* **96**, 6261–6266
13. Csernok, E., Szymkowiak, C.H., Mistry, N., Daha, M.R., Gross, W.L., and Kekow, J. (1996) Transforming growth factor-beta (TGF-β) expression and interaction with proteinase 3 (PR3) in anti-neutrophil cytoplasmic antibody (ANCA)-associated vasculitis. *Clin. Exp. Immunol.* **105**, 104–111
14. Gabay, J.E., Scott, R.W., Campanelli, D., Griffith, J., Wilde, C., Marra, M.N., Seeger, M., and Nathan, C.F. (1989) Antibiotic proteins of human polymorphonuclear leukocytes. *Proc. Natl. Acad. Sci. USA.* **86**, 5610–5614
15. Berger, S.P., Seelen, M. A. J., Hiemstra, P.S., Gerritsma, J. S. J., Heemskerk, E., van der Woude, F.J., and Daha, M.R. (1996) Proteinase 3, the major autoantigen of Wegener's granulomatosis, enhances IL-8 production by endothelial cells *in vitro*. *J. Am. Soc. Nephrol.* **7**, 694–701
16. Tal, T., Michaela, S., and Aviram, I. (1998) Cationic proteins of neutrophil azurophilic granules: protein-protein interaction and blockade of NADPH oxidase activation. *J. Leuk. Biol.* **63**, 305–311
17. Franzoso, G., Biswas, P., Poli, G., Carlson, L.M., Brown, K.D., Tomita-Yamaguchi, M., Fauci, A.S., and Siebenlist, U. (1994) A family of serine proteases expressed exclusively in myelo-monocytic cells specifically processes the nuclear factor-kB subunit p65 *in vitro* and may impair human immunodeficiency virus replication in these cells. *J. Exp. Med.* **180**, 1445–1456
18. Spector, N.L., Hardy, L., Ryan, C., Miller, W.H.Jr, Humes, J.L., Nadler, L.M., and Luedke, E. (1995) 28-kDa mammalian heat shock protein, a novel substrate of a growth regulatory protease involved in differentiation of human leukemia cells. *J. Biol. Chem.* **270**, 1003–1106
19. Rao, J., Zhang, F., Donnelly, R.J., Spector, N.L., and Studzinski, G.P. (1998) Truncation of Sp1 transcription factor by myeloblastin in undifferentiated HL60 cells. *J. Cell Physiol.* **175**, 121–128
20. Sköld, S., Rosberg, B., Gullberg, U., and Olofsson, T. (1999) A secreted proform of neutrophil proteinase 3 regulates the proliferation of granulopoietic progenitor cells. *Blood* **93**, 849–856
21. Molldrem, J.J., Clave, E., Jiang, Y.Z., Mavroudix, D., Raptis, A., Hensel, N., Agarwala, V., and Barrett, A.J. (1997) Cytotoxic T lymphocytes specific for a nonpolymorphic proteinase 3 peptide preferentially inhibit chronic myeloid leukemia colony-forming units. *Blood* **90**, 2529–2534
22. Molldrem, J.J., Lee, P.P., Kant, S., Wieder, E., Jiang, W., Lu, S., Wang, C., and Davis, M.M. (2003) Chronic myelogenous leukemia shapes host immunity by selective deletion of high-avidity leukemia-specific T cells. *J. Clin. Invest.* **111**, 639–647
23. Jenne, D.E., Tschopp, J., Lüdemann, J., Utecht, B., and Gross, W.L. (1990) Wegener's autoantigen decoded. *Nature* **346**, 520
24. Russell, K.A. and Specks, U. (2001) Are antineutrophil cytoplasmic antibodies pathogenic? Experimental approaches to understand the antineutrophil cytoplasmic antibody phenomenon. *Rheum. Dis. Clin. North. Am.* **27**, 815–832
25. Savage, C.O., Harper, L., and Holland, M. (2002) New findings in pathogenesis of antineutrophil cytoplasm antibody- associated vasculitis. *Curr. Opin. Rheumatol.* **14**, 15–22

26. Bini, P., Gabay, J.E., Teitel, A., Melchior, M., Zhou, J.-L., and Elkon, K.B. (1992) Antineutrophil cytoplasmic autoantibodies in Wegener's granulomatosis recognize conformational epitopes on proteinase 3. *J. Immunol.* **149**, 1409–1415
27. Rudd, P.M., Elliott, T., Cresswell, P., Wilson, I.A., and Dwek, R.A. (2001) Glycosylation and the immune system. *Science* **291**, 2370–2376
28. Fiedler, K. and Simons, K. (1995) The role of N-glycans in the secretory pathway. *Cell* **81**, 309–312
29. Helenius, A. and Aebi, M. (2001) Intracellular functions of N-linked glycans. *Science* **291**, 2364–2369
30. Campanelli, D., Melchior, M., Fu, Y., Nakata, M., Shuman, H., Nathan, C., and Gabay, J.E. (1990) Cloning of cDNA for proteinase 3: a serine protease, antibiotic, and autoantigen from human neutrophils. *J. Exp. Med.* **172**, 1709–1715
31. Jenne, D.E., Fröhlich, L., Hummel, A.M., and Specks, U. (1997) Cloning and functional expression of the murine homologue of proteinase 3: implications for the design of murine models of vasculitis. *FEBS Lett.* **408**, 187–190
32. Bode, W., Wei, A.Z., Huber, R., Meyer, E., Travis, J., and Neumann, S. (1986) X-ray crystal structure of the complex of human leukocyte elastase (PMN elastase) and the third domain of the turkey ovomucoid inhibitor. *Embo. J.* **5**, 2453–2458
33. Fujinaga, M., Chernaia, M.M., Halenbeck, R., Koths, K., and James, M.N. (1996) The crystal structure of PR3, a neutrophil serine proteinase antigen of Wegener's granulomatosis antibodies. *J. Mol. Biol.* **261**, 267–278
34. Altmann, F., Staudacher, E., Wilson, I.B., and Marz, L. (1999) Insect cells as hosts for the expression of recombinant glycoproteins. *Glycoconj. J.* **16**, 109–123
35. Chang, G.D., Chen, C.J., Lin, C.Y., Chen, H.C., and Chen, H. (2003) Improvement of glycosylation in insect cells with mammalian glycosyltransferases. *J. Biotechnol.* **102**, 61–71
36. Sun, J., Fass, D.N., Hudson, J.A., Viss, M.A., Wieslander, J., Homburger, H.A., and Specks, U. (1998) Capture-ELISA based on recombinant PR3 is sensitive for PR3-ANCA testing and allows detection of PR3 and PR3-ANCA/PR3 immunecomplexes. *J. Immunol. Methods* **211**, 111–123
37. Sommarin, Y., Rasmussen, N., and Wieslander, J. (1995) Characterization of monoclonal antibodies to proteinase 3 and application in the study of epitopes for classical anti-neutrophil cytoplasm antibodies. *Exp. Nephrol.* **3**, 249–256
38. van der Geld, Y.M., Limburg, P.C., and Kallenberg, C.G. (1999) Characterization of monoclonal antibodies to proteinase 3 (PR3) as candidate tools for epitope mapping of human anti-PR3 autoantibodies. *Clin. Exp. Immunol.* **118**, 487–496
39. Butterfield, J.H., Weiler, D., Dewald, G., and Gleich, G.J. (1988) Establishment of an immature mast cell line from a patient with mast cell leukemia. *Leukemia. Res.* **12**, 345–355
40. Specks, U., Fass, D.N., Fautsch, M.P., Hummel, A.M., and Viss, M.A. (1996) Recombinant human proteinase 3, the Wegener's autoantigen, expressed in HMC-1 cells is enzymatically active and recognized by c-ANCA. *FEBS Lett.* **390**, 265–270
41. Horton, R.M., Hunt, H.D., Ho, S.N., Pullen, J.K., and Pease, L.R. (1989) Engineering hybrid genes without the use of restriction enzymes: gene splicing by overlap extension. *Gene* **77**, 61–68
42. Specks, U., Wiegert, E.M., and Homburger, H.A. (1997) Human mast cells expressing recombinant proteinase 3 (PR3) as substrate for clinical testing for anti-neutrophil cytoplasmic antibodies (ANCA). *Clin. Exp. Immunol.* **109**, 286–295
43. Sun, J., Fass, D.N., Viss, M.A., Hummel, A.M., Tang, H., Homburger, H.A., and Specks, U. (1998) A proportion of proteinase 3-specific anti-neutrophil cytoplasmic antibodies only react with proteinase 3 after cleavage of its N-terminal activation dipeptide. *Clin. Exp. Immunol.* **114**, 320–326
44. McDowell, E.M. and Trump, B.F. (1976) Histologic fixatives suitable for diagnostic light and electron microscopy. *Arch. Pathol. Lab. Med.* **100**, 405–414
45. Spurr, A.R. (1969) A low-viscosity epoxy resin sembedding medium for electron microscopy. *J. Ultrastruct. Res.* **26**, 31–43
46. Allen, G. (1989) Determination of peptide sequences. In sequencing of proteins and peptides, pp. 207–293
47. Kirszbaum, L., Bozas, S.E., and Walker, I.D. (1992) SP-40,40, a protein involved in the control of the complement pathway, possesses a unique array of disulphide bridges. *FEBS Lett.* **297**, 70–76
48. Borregaard, N., Heiple, J.M., Simons, E.R., and Clark, R.A. (1983) Subcellular localization of the *b*-cytochrome component of the human neutrophil microbicidal oxidase: translocation during activation. *J. Cell. Biol.* **97**, 52–61
49. Rao, N.V., Rao, G.V., Marshall, B.C., and Hoidal, J.R. (1996) Biosynthesis and processing of proteinase 3 in U937 cells. *J. Biol. Chem.* **271**, 2972–2978
50. Garwicz, D., Lindmark, A., Hellmark, T., Gladh, M., Jögl, J., and Gullberg, U. (1997) Characterization of the processing and granular targeting of human proteinase 3 after transfection to the rat RBL or the murine 32D leukemic cell lines. *J. Leukoc. Biol.* **61**, 113–123
51. Garwicz, D., Lindmark, A., and Gullberg, U. (1995) Human cathepsin G lacking functional glycosylation site is proteolytically processed and targeted for storage in granules after transfection to the rat basophilic/mast cell line RBL or the murine myeloid cell line 32D. *J. Biol. Chem.* **270**, 28413–28418
52. Witko-Sarsat, V., Halbwachs-Mecarelli, L., Almeida, R.P., Nusbaum, P., Melchior, M., Jamaleddine, G., Lesavre, P., Deschamps-Latscha, B., and Gabay, J.E. (1996) Characterization of a recombinant proteinase 3, the autoantigen in Wegener's granulomatosis and its reactivity with anti-neutrophil cytoplasmic autoantibodies. *FEBS Letters.* **382**, 130–136
53. Russell, K.A., Fass, D.N., and Specks, U. (2001) Antineutrophil cytoplasmic antibodies reacting with the pro form of proteinase 3 and disease activity in patients with Wegener's granulomatosis and microscopic polyangiitis. *Arthritis Rheum.* **44**, 463–468
54. Fillit, H., Shibata, S., Sasaki, T., Spiera, H., Kerr, L.D., and Blake, M. (1993) Autoantibodies to the protein core of vascular basement membrane heparan sulfate proteoglycan in systemic lupus erythematosus. *Autoimmunity* **14**, 243–249
55. Casciola-Rosen, L., Andrade, F., Ulanet, D., Wong, W.B., and Rosen, A. (1999) Cleavage by granzyme B is strongly predictive of autoantigen status: implications for initiation of autoimmunity. *J. Exp. Med.* **190**, 815–826
56. Gahring, L., Carlson, N.G., Meyer, E.L., and Rogers, S.W. (2001) Granzyme B proteolysis of a neuronal glutamate receptor generates an autoantigen and is modulated by glycosylation. *J. Immunol.* **166**, 1433–1438
57. McCormick, T.S. and Rowland, E.C. (1993) Trypanosoma cruzi: recognition of a 43-kDa muscle glycoprotein by autoantibodies present during murine infection. *Exp. Parasitol.* **77**, 273–281
58. Seetharamaiah, G.S., Dallas, J.S., Patibandla, S.A., Thotakura, N.R., and Prabhakar, B.S. (1997) Requirement of glycosylation of the human thyrotropin receptor ectodomain for its reactivity with autoantibodies in patients' sera. *J. Immunol.* **158**, 2798–2804
59. Blass, S., Meier, C., Vohr, H.W., Schwochau, M., Specker, C., and Burmester, G.R. (1998) The p68 autoantigen characteristic of rheumatoid arthritis is reactive with carbohydrate epitope specific autoantibodies. *Ann. Rheum. Dis.* **57**, 220–225